Retrolinkin cooperates with endophilin A1 to mediate BDNF–TrkB early endocytic trafficking and signaling from early endosomes

Xiuping Fu[a,b], Yanrui Yang[a,*], Chenchang Xu[a,b,*], Yang Niu[a,b], Tielin Chen[c], Qin Zhou[c], and Jia-Jia Liu[a]

[a]Key Laboratory of Molecular and Developmental Biology, Institute of Genetics and Developmental Biology, Chinese Academy of Sciences, Beijing 100101, China; [b]Graduate School, Chinese Academy of Sciences, Beijing 100039, China; [c]Core Facility of Genetically Engineered Mice, State Key Laboratory of Biotherapy and Cancer Center, West China Hospital, Sichuan University, Chengdu 610041, China

ABSTRACT **Brain-derived neurotrophic factor (BDNF) binds to its cell surface receptor TrkB to regulate differentiation, development, synaptic plasticity, and functional maintenance of neuronal cells. Binding of BDNF triggers TrkB dimerization and autophosphorylation, which provides docking sites for adaptor proteins to recruit and activate downstream signaling molecules. The molecular mechanisms underlying BDNF–TrkB endocytic trafficking crucial for spatiotemporal control of signaling pathways remain to be elucidated. Here we show that retrolinkin, a transmembrane protein, interacts with endophilin A1 and mediates BDNF-activated TrkB (pTrk) trafficking and signaling in CNS neurons. We find that activated TrkB colocalizes and interacts with the early endosome marker APPL1. Both retrolinkin and endophilin A1 are required for BDNF-induced dendrite development and acute extracellular signal-regulated kinase activation from early endosomes. Suppression of retrolinkin expression not only blocks BDNF-triggered TrkB internalization, but also prevents recruitment of endophilin A1 to pTrk vesicles trafficking through APPL1-positive endosomes. These findings reveal a novel mechanism for BDNF–TrkB to regulate signaling both in time and space through a specific membrane trafficking pathway.**

Monitoring Editor
Jean E. Gruenberg
University of Geneva

Received: Apr 8, 2011
Revised: Jul 6, 2011
Accepted: Aug 5, 2011

INTRODUCTION

The neurotrophin family of target-derived growth factors is crucial for neuronal development, survival, differentiation, and plasticity (Huang and Reichardt, 2001; Lu, 2003). Members of this family include nerve growth factor (NGF), brain-derived neurotrophic factor (BDNF), neurotrophin-3 (NT-3), and NT-4/5 (Huang and Reichardt, 2003; Segal, 2003). The neurotrophins elicit signaling events by binding the cell-surface Trk receptor tyrosine kinases (RTKs) and triggering their dimerization and autophosphorylation, which provides docking sites for adaptor and effector proteins to activate multiple intracellular signaling cascades (Huang and Reichardt, 2003; Segal, 2003). Binding of the ligand also triggers internalization of the ligand–receptor signal complex, which, in turn, can be transported in the form of signaling endosomes from the nerve terminal to cell body to mediate more signaling events (Kaplan and Miller, 2000; Huang and Reichardt, 2003; Segal, 2003; Philippidou *et al.*, 2011).

The spatiotemporal regulation of signaling cascades is crucial for cellular responses to RTKs and their cognate ligands. For example, NGF induces sustained activation of extracellular signal-regulated kinase (ERK) and promotes differentiation of PC12 cells, whereas epidermal growth factor (EGF) induces transient ERK activation and provokes cell proliferation (Traverse *et al.*, 1992; Nguyen *et al.*, 1993). It was reported that PDZ-GEF1, a GDP/GTP exchange factor (GEF) for Rap1, binds to activated Trk at late endosomes and induces sustained activation of both Rap1 and ERK, as well as neurite outgrowth (Hisata *et al.*, 2007). It was also reported that the kinetics of Trk recycling to the plasma membrane and their subcellular localization plays a role in the spatiotemporal regulation of distinct downstream targets (Chen *et al.*, 2005; Huang *et al.*, 2009). However, the mechanisms for membrane trafficking of neurotrophin

This article was published online ahead of print in MBoC in Press (http://www.molbiolcell.org/cgi/doi/10.1091/mbc.E11-04-0308) on August 17, 2011.

*These authors contributed equally to this work.

Address correspondence to: Jia-Jia Liu (jjliu@genetics.ac.cn).

Abbreviations used: coIP, coimmunoprecipitation; DIV, days in vitro; RTK, receptor tyrosine kinase.

signal complexes to regulate the specificity and duration of signal transduction remain largely elusive.

Previous studies found that retrolinkin (also known as Tmem108, GenBank accession number NP_848753), a transmembrane protein, mediates retrograde axonal transport in sensory neurons through interaction with the dynein/dynactin cargo adaptor BPAG1n4 (Liu *et al.*, 2007). In this study, we present evidence that retrolinkin functions in the endocytic trafficking of BDNF–TrkB and mediates BDNF-triggered ERK signaling in CNS neurons. We demonstrate that retrolinkin is a binding partner of endophilin A1 and that both proteins are required for BDNF-induced dendrite outgrowth. Knockdown of retrolinkin but not endophilin A1 inhibits receptor-mediated endocytosis at the neuronal plasma membrane. We further demonstrate that suppression of retrolinkin or endophilin A1 activity specifically inhibits acute activation of ERK from early endosomes and that endophilin A1 works downstream of retrolinkin in the BDNF–TrkB endocytic trafficking pathway. Our findings identify a requirement of BDNF-induced acute ERK activation for dendrite development and provide novel insights into the molecular mechanisms for membrane trafficking to regulate the specificity of RTK-mediated signal transduction.

RESULTS

Knockdown of retrolinkin impairs dendrite development

Immunohistochemical analysis using antibodies against retrolinkin revealed that it is expressed not only in sensory neurons of the peripheral nervous system, but also in the CNS, including the cerebral cortex, hippocampus, and cerebellum (Figure 1A). Immunofluorescence staining of cultured hippocampal neurons detected retrolinkin in both axons and somatodendritic regions (Figure 1B). Quantitative analysis of fluorescence signal intensity revealed that retrolinkin is primarily located in dendrites (Figure 1C). These findings prompted us to investigate its function(s) in CNS neurons, especially in their dendrite development.

To investigate retrolinkin function in CNS neurons, we suppressed its expression by short hairpin RNA (shRNA)–mediated knockdown in cultured hippocampal neurons on days in vitro (DIV) 1 and monitored their morphology on DIV5 (see Supplemental Figure S1 for knockdown efficiency. Because shRNA#1 and #2 knocked down retrolinkin expression to similar levels, we used shRNA#1 throughout this study). Depletion of retrolinkin resulted in decreased length of dendrites, with no obvious change in soma size, axon length (Figure 1, D and E), and branching or the number of dendrites (Supplemental Figure S2). The dendrite outgrowth defect was rescued by coexpression of RNA interference (RNAi)–resistant retrolinkin (Figure 1, D and E), indicating that the knockdown effect was specific.

Retrolinkin interacts directly with endophilin A1, which is also required for dendrite development

To investigate retrolinkin function in dendrite development of CNS neurons, we set out to search for its interaction partners other than the sensory neuron–specific BPAG1n4 protein with a yeast two-hybrid screen of a human fetal brain cDNA library using human retrolinkin as bait. One of 20 positive clones was found to encode for the carboxyl-terminus (amino acids 182–352) of endophilin A1 (Figure 2, A and B), which is a member of the endophilin family and plays a role in clathrin-mediated endocytosis of synaptic vesicles (Ringstad *et al.*, 1999). To verify the interaction, we performed a coimmunoprecipitation (coIP) assay using mouse brain lysates and detected endophilin A1 in the immunoprecipitates of retrolinkin (Figure 2C; see also Supplemental Figure S3 showing antibody specificity); conversely, antibodies to endophilin A1 coimmunoprecipitated retrolinkin (Figure 2C). Glutathione *S*-transferase (GST) pull down with the mouse retrolinkin amino-terminus (amino acids 31–460) fused to GST also identified endophilin A1 as its binding partner (Figure 2D). Endophilins contain an SH3 domain that interacts with proline-rich domains (PRDs) of other proteins (Reutens and Begley, 2002). Indeed, the SH3 but not the BAR domain of endophilin A1 bound to retrolinkin (Figure 2E). Furthermore, we identified the PRD domain (amino acids 31–169) of retrolinkin as its binding site for endophilin A1 (Figure 2F).

To further verify the interaction, we performed double immunofluorescence staining of cultured hippocampal neurons after 7 DIV and detected colocalization of endophilin A1 and retrolinkin on vesicular structures in neurites (Figure 2G). Of interest, in contrast to retrolinkin, which was primarily located in dendrites (Figure 1, B and C), endophilin A1 was more evenly distributed (Supplemental Figure S3, B and C).

Finally, we performed double immunogold labeling of mouse hippocampal ultrathin sections with antibodies to retrolinkin and endophilin A1 and detected colabeling of retrolinkin and endophilin A1–specific gold particles on vesicular structures (Figure 2, H–I′). From three independent trials, 43 ± 2.4% of retrolinkin-immunolabeled structures were colabeled with antibodies to endophilin A1; conversely, 63 ± 6.7% of endophilin A1–positive structures were also positive for retrolinkin (Figure 2K). No significant labeling was detected in negative controls using secondary antibodies only (Figure 2J). Taken together, these results indicate that retrolinkin directly interacts with endophilin A1.

Next we asked whether endophilin A1 functions in the same biological process as retrolinkin. In endophilin A1–depleted hippocampal neurons (see Supplemental Figure S1 for knockdown efficiency), similar to retrolinkin knockdown, the total length of dendrites was decreased (Figure 1, D and E), suggesting that it is also involved in dendrite outgrowth. The dendrite outgrowth defect was partially rescued by coexpression of RNAi-resistant endophilin A1 (Figure 1, D and E), indicating that the knockdown effect was specific. A slight decrease in axon length was also observed in endophilin A1–depleted neurons (Figure 1, D and E) but was statistically insignificant ($p > 0.05$).

Retrolinkin and endophilin A1 are required for BDNF-induced dendrite outgrowth and acute activation of ERK

Having found that both retrolinkin and endophilin A1 are required for dendrite outgrowth, we asked which specific regulatory factor(s) might be involved in this process. Many extrinsic factors, including neurotrophins, regulate neurite morphogenesis (Marshall, 1995; McAllister *et al.*, 1997; Xu *et al.*, 2000; Jan and Jan, 2003). Previous studies established that BDNF plays an important role in regulating dendritic development of cortical neurons (Marshall, 1995; Niblock *et al.*, 2000) and that clathrin-dependent endocytosis of TrkB is required for BDNF-induced dendritic growth (Zheng *et al.*, 2008). To investigate mechanistic role(s) of retrolinkin and endophilin A1 in dendrite development, we examined whether BDNF-induced dendritogenesis requires their activities. Hippocampal neurons were treated with BDNF on DIV1 and neuronal morphology was observed on DIV5. Consistent with previous studies (McAllister *et al.*, 1995; Piontek *et al.*, 1999), BDNF treatment caused a significant increase in the total dendritic length of control neurons (Figure 3, A and B). In contrast, BDNF did not promote dendrite extension of retrolinkin-depleted neurons (Figure 3, A and B), indicating that retrolinkin is required for BDNF-stimulated dendrite outgrowth. Depletion of endophilin A1 had a similar effect (Figure 3, A and B).

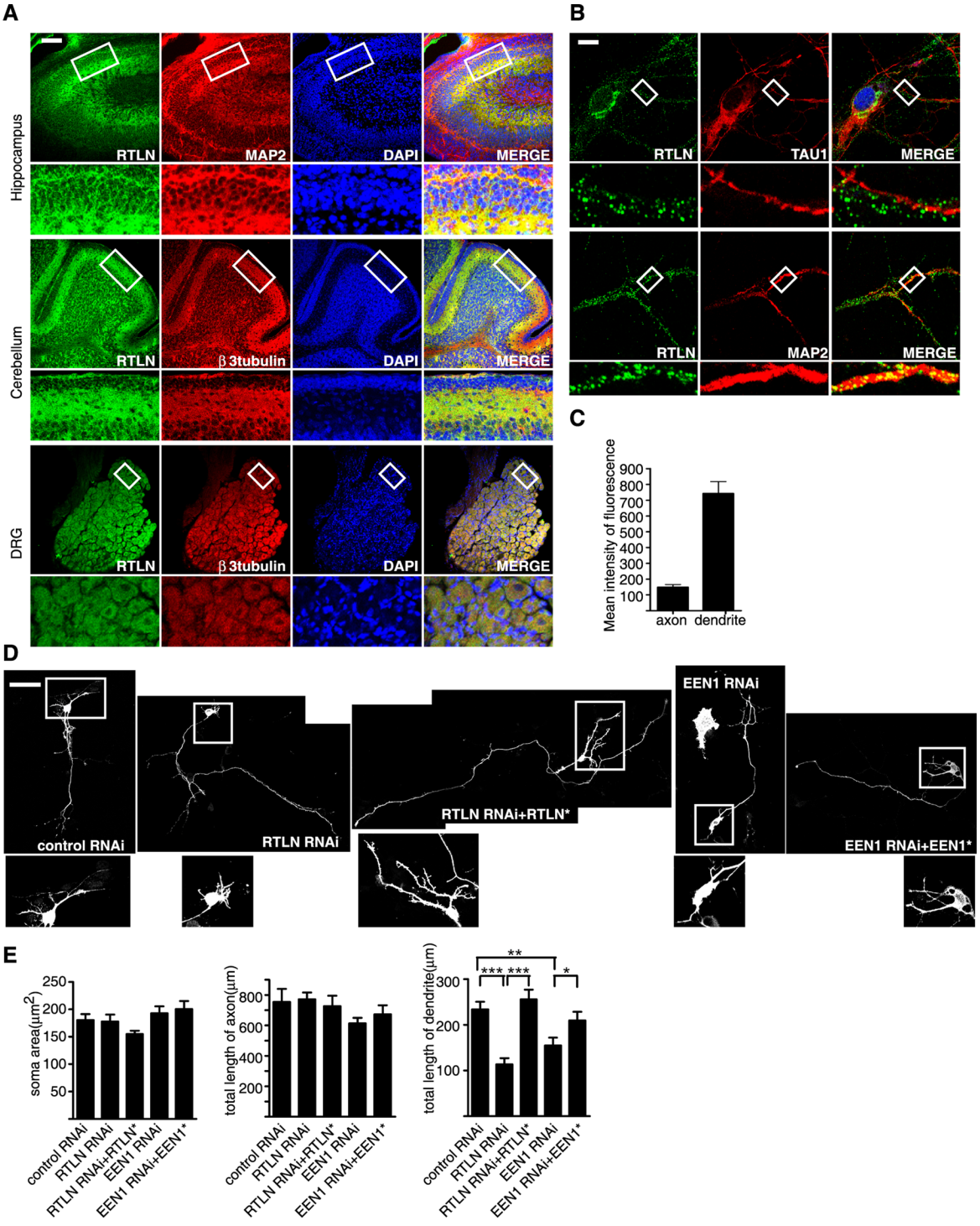

FIGURE 1: Retrolinkin is preferentially expressed in dendrites of CNS neurons and is required for dendrite outgrowth. (A) Immunohistochemical analysis of retrolinkin (labeled as RTLN) expression in the brain cortex, cerebellum, and dorsal root ganglia (DRG) of adult mouse. Regions within white boxes (top) are shown at higher magnification (bottom). Note that retrolinkin was strongly expressed in the dendrites of hippocampus and the molecular layer enriched of Purkinje cell dendrites in cerebellum. Scale bar, 100 μm. (B) Cultured hippocampal neurons were fixed and immunostained for endogenous retrolinkin (green) and the dendritic marker MAP2 (red) or the axonal marker TAU1 (red). Scale bar, 10 μm. (C) Background-subtracted, mean intensity of retrolinkin fluorescence in primary axons and dendrites. Measurement of fluorescence intensity is expressed in arbitrary units per square area in both axons and dendrites. All images were obtained in the same settings below saturation at a resolution of 1024 × 1024 pixels (12 bits) (n = 16; ***p < 0.001). (D) Hippocampal neurons were transfected at DIV1 with shRNA constructs coexpressing red fluorescent protein (RFP) and shRNA or cotransfected with shRNA and RNAi-resistant expression constructs (indicated by asterisk) and fixed at DIV5, followed by immunostaining with the anti-RFP antibody. Scale bar, 100 μm. (E) Quantification of soma area and neurite length per transfected neuron. Shown are average soma area (± SEM) and neurite length (± SEM) of 40–60 neurons (*p < 0.05; **p < 0.01).

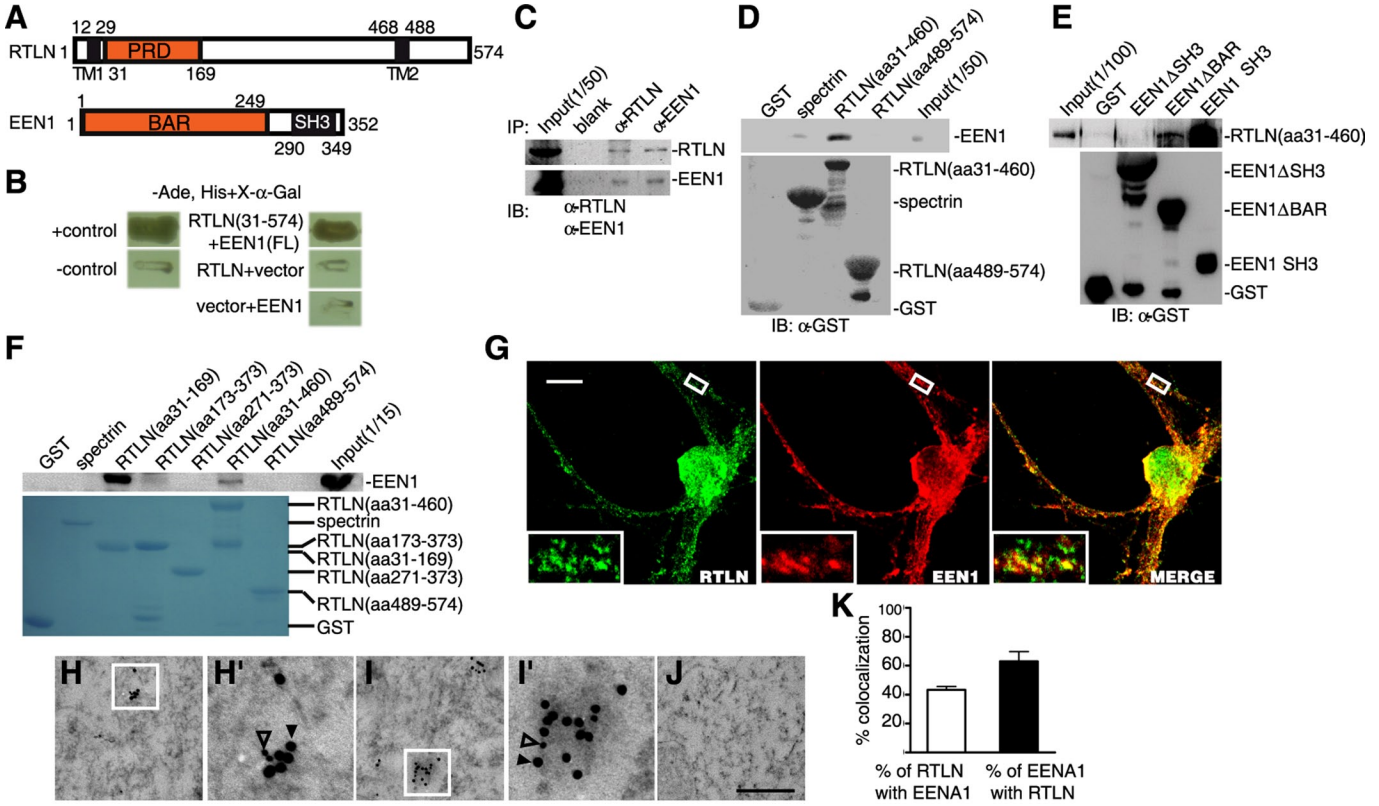

FIGURE 2: Retrolinkin interacts with endophilin A1 (labeled as EEN1) directly. (A) Schematic representation of the domain structures of retrolinkin and endophilin A1. TM, transmembrane regions. (B) Yeast two-hybrid assay showing the interaction of retrolinkin (aa 31–574) with full-length (FL) endophilin A1. Interaction of the fusion proteins was detected by growth of yeast cells in the absence of adenine and histidine (−Ade, His) and the α-galactosidase colorimetric assay as described in *Materials and Methods*. (C) Lysates from adult mouse brain were subjected to coIP with antibodies to retrolinkin or endophilin A1, followed by Western blotting analysis. IB, immunoblotting. (D) In vitro binding between endophilin A1 and the N-terminus of retrolinkin. Recombinant His-tagged endophilin A1 was incubated with GST-fusion proteins conjugated to glutathione–Sepharose. GST alone and GST-βIII spectrin served as controls. (E) The retrolinkin-binding site maps to the SH3 domain of endophilin A1. Shown is a GST pull-down assay using His-tagged retrolinkin (aa 31–460) and GST-tagged endophilin A1 fragments. (F) The endophilin A1–binding site maps to the PRD domain of retrolinkin. Shown is a GST pull-down assay using lysates from 293 cells overexpressing myc-tagged endophilin A1. A GST tag was fused to each retrolinkin fragment at the N-terminus of the protein. (G) Cultured hippocampal neurons were immunostained with antibodies to retrolinkin and endophilin A1. Boxed regions are shown at higher magnification. Scale bar, 10 μm. (H, I) Representative examples of double immunogold labeling of retrolinkin (18 nm, solid triangle) and endophilin A1 (12 nm, open triangle). (H′, I′) Higher magnification of boxed areas in H and I, respectively. (J) Negative control with secondary antibodies only. Scale bar, 350 nm in H–J, and 100 nm in H′, I′. (K) Quantification of the colocalization between retrolinkin and endophilin A1 in immunoEM. Data represent means ± SEM (n = 3).

To investigate roles of retrolinkin and endophilin A1 in BDNF signaling, we examined the kinetics of BDNF-induced phosphorylation of TrkB. Western blotting analysis detected no change in the kinetics of TrkB phosphorylation in neurons depleted of retrolinkin or endophilin A1 (Figure 3, C and E), indicating that neither protein is involved in BDNF-triggered TrkB activation. Formation of the neurotrophin-Trk signal complex initiates its endocytosis and subsequent signaling events (Ehlers *et al.*, 1995; Grimes *et al.*, 1996; Heerssen and Segal, 2002) regulated by mitogen-activated protein kinases (MAPKs), phosphatidylinositol 3-kinase/Akt, and phospholipase-C-γ (PLC-γ) (Huang and Reichardt, 2003; Dijkhuizen and Ghosh, 2005). To identify the cellular pathway(s) in which retrolinkin and endophilin A1 are involved, we investigated the phosphorylation kinetics of these downstream effectors in BDNF-stimulated neurons. Immunoblotting analysis detected BDNF-induced activation of the MAPK ERK1/2 as early as 5 min (Supplemental Figure S4), with its phosphorylation levels peaking at 30 min and decreasing thereafter (Figure 3, D and E, and Supplemental Figure S4). The phosphorylation kinetics of Akt and PLC-γ showed a similar pattern to that of ERK1/2 (Figure 3, D and E, and Supplemental Figure S4). Thus BDNF induces both acute and prolonged activation of all three signaling pathways in CNS neurons. We then examined activation of the signaling molecules in neurons depleted of retrolinkin or endophilin A1. Immunoblotting analysis showed that depletion of either protein did not have an obvious effect on the kinetics of Akt activation or that of PLC-γ (Figure 3, D and E). In contrast, acute activation of ERK1/2 was impaired, whereas levels of phosphorylated ERK1/2 (pERK1/2) at 60 min after BDNF addition were not affected in cells depleted of either protein (Figure 3, D and E), indicating that they selectively regulate BDNF-induced acute ERK1/2 activation.

Moreover, confocal analysis detected colocalization between retrolinkin and pERK1/2 but not pAkt on vesicular structures upon BDNF treatment (Figure 3, F–H). Similarly, colocalization between endophilin A1 and pERK1/2 but not pAkt on vesicular structures was

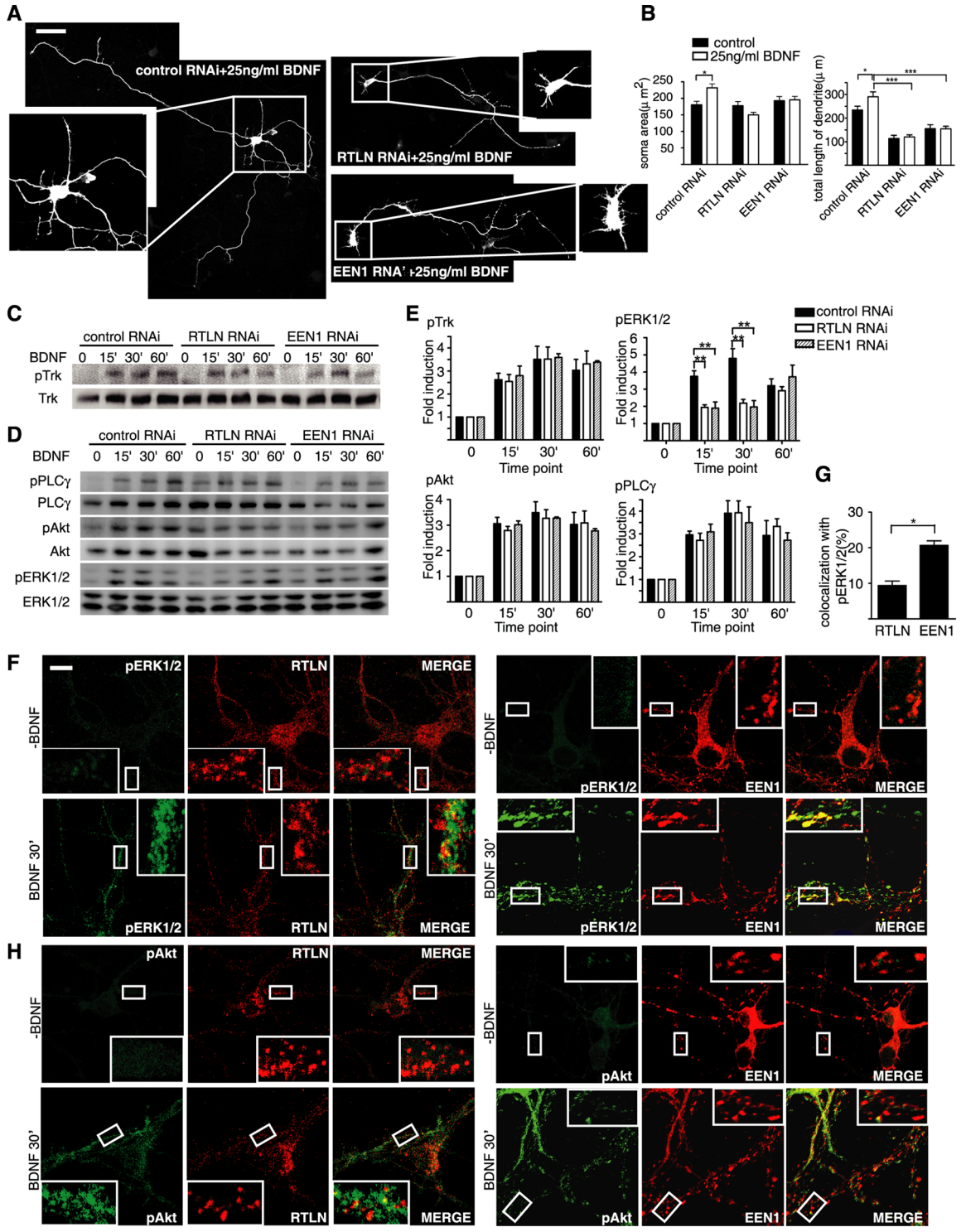

FIGURE 3: Retrolinkin and endophilin A1 are required for BDNF-induced dendritic outgrowth and acute ERK activation. (A) Neurons transfected with shRNA constructs at DIV1 were cultured for 4 d in the presence of BDNF (25 ng/ml) and allowed to extend axons and dendrites. Scale bar, 100 μm. (B) Quantification of soma area and the length of dendrites per transfected neuron in A. Shown are average soma area (± SEM) and dendrite length (± SEM) of 40–60 neurons (*$p < 0.05$; ***$p < 0.001$). (C, D) Cortical neurons infected with *Lentivirus* expressing shRNA were treated with BDNF for different periods and lysed. Total and phosphorylated protein levels were examined by Western blotting. (E) Quantitative analysis of the immunoblot bands. Average pTrk, pERK1/2, pAkt, and pPLCγ levels were normalized to levels detected at the 0-min time point and represented as fold induction. Data represent means ± SEM (**$p < 0.01$, $n = 5$). (F) DIV10 hippocampal neurons were starved for 2 h, treated with 25 ng/ml BDNF, fixed, and immunostained with antibodies to pERK1/2 and retrolinkin or endophilin A1. (G) Quantification of the colocalization between pERK1/2 and endophilin A1 or retrolinkin. Data represent means ± SEM ($n = 12–20$) (*$p < 0.05$). (H) Same as F, except that neurons were immunostained with antibodies to pAkt and retrolinkin or endophilin A1. Scale bar, 10 μm. EEN1, endophilin A1; RTLN, retrolinkin.

detected upon BDNF treatment (Figure 3, F–H). These results not only indicate that retrolinkin and endophilin A1 play a regulatory role in BDNF-induced ERK activation, but they also suggest their involvement in ERK signaling from vesicles.

Retrolinkin, not endophilin A1, is required for BDNF-triggered TrkB endocytosis in CNS neurons

Different membrane trafficking pathways elicit distinct signaling pathways and cellular responses. Because retrolinkin and endophilin A1 selectively regulate BDNF-triggered ERK signaling kinetics, we reasoned that they might play a role in cell surface entry or trafficking pathways for the BDNF–TrkB signal complex to differentially regulate downstream signaling cascades. To investigate retrolinkin and endophilin A1 function(s) in BDNF–TrkB trafficking, first we performed immunofluorescence staining to detect colocalization of pTrk with both retrolinkin and endophilin A1 on vesicular structures in hippocampal neurons upon BDNF stimulation. The results showed that both proteins associated with vesicles carrying pTrk (Figure 4A). Double immunogold labeling of mouse hippocampal sections also revealed that both retrolinkin and endophilin A1 colocalized with pTrk on vesicular structures (Figure 4, B–E′). Quantitative analyses showed that 39 ± 6.8% of retrolinkin-positive structures were colabeled with antibodies to pTrk; conversely, 69 ± 5.1% of pTrk-positive vesicular structures were also positive for retrolinkin (Figure 4G). Meanwhile, 36 ± 1.7% of endophilin A1-immunolabeled structures were colabeled with antibodies to pTrk; conversely, 58 ± 1.7% of pTrk-positive structures were also positive for endophilin A1 (Figure 4H). Collectively, these findings implicate the involvement of retrolinkin and endophilin A1 in BDNF–TrkB membrane trafficking.

Because endophilin A1 is involved in multiple stages of clathrin-mediated endocytosis (Ringstad *et al.*, 1999; Gad *et al.*, 2000; Guichet *et al.*, 2002; Verstreken *et al.*, 2002, 2003; Schuske *et al.*, 2003), we reasoned that retrolinkin might cooperate with endophilin A1 to function in endocytosis. To test this possibility, we examined BDNF-triggered TrkB internalization in hippocampal neurons using a surface biotinylation assay. BDNF-treated cells were incubated with biotin, and biotinylated surface TrkB was affinity purified with streptavidin-conjugated beads. The surface TrkB levels decreased after BDNF stimulation in control neurons as measured by Western blotting; in contrast, less TrkB was internalized in retrolinkin-depleted cells (Figure 4I). It was surprising that no decrease in TrkB endocytosis was detected in cells depleted of endophilin A1 (Figure 4I). Note that although an increase in TrkB endocytosis was observed in endophilin A1–depleted cells, this effect is statistically insignificant, indicating that only retrolinkin is required for BDNF-triggered TrkB internalization.

To visualize receptor-mediated endocytosis and confirm results from the surface biotinylation assay, we overexpressed FLAG-tagged TrkB in hippocampal neurons by transient transfection (Supplemental Figure S5) and monitored its internalization with bound fluorescein isothiocyanate (FITC)–conjugated anti-FLAG antibodies. Confocal microscopy revealed that BDNF-stimulated endocytosis of FLAG-TrkB was abolished in retrolinkin- but not endophilin A1–depleted neurons (Figure 4J). To determine whether retrolinkin also functions in receptor-mediated endocytosis of other ligands, we performed an uptake assay using Alexa 488–conjugated transferrin molecules. Similarly, internalization of transferrin through its binding to transferrin receptor on the cell surface was greatly inhibited in retrolinkin- but not endophilin A1–depleted neurons (Figure 4K). Taken together, these results indicate that retrolinkin, not endophilin A1, is required for receptor-mediated endocytosis in CNS neurons.

BDNF-activated TrkB traffics through APPL1-positive endosomes

It was reported that the endocytic vesicles of the NGF–TrkA signal complex form signaling endosomes to regulate downstream signaling events. NGF induces acute activation of ERK1/2 on early endosomes in sensory neurons (Delcroix *et al.*, 2003). Although endophilin A1 is not required for BDNF-triggered TrkB endocytosis, depletion of endophilin A1 impaired the acute activation of ERK1/2. Therefore, we reasoned that retrolinkin and endophilin A1 might cooperate to regulate BDNF–TrkB early endocytic trafficking and signaling from early endosomes. To investigate whether BDNF–TrkB also signals from early endosomes, first we examined colocalization of pTrk with the early endosome antigen (EEA1) marker. It was surprising that immunostaining and immuno–electron microscopy (immunoEM) analyses of neurons detected little colocalization between pTrk and EEA1 (Supplemental Figure S6), suggesting that the BDNF–TrkB complex might reach endosomes via an EEA1-independent pathway. Previous studies found that the membrane adaptor protein APPL1 binds to membrane receptors, including TrkA (Lin *et al.*, 2006; Mao *et al.*, 2006), and APPL1 endosomes serve as platforms for the assembly of signaling complexes regulating the MAPK and Akt pathways (Yang *et al.*, 2003; Lin *et al.*, 2006; Varsano *et al.*, 2006; Schenck *et al.*, 2008). A recent study reported that APPL1 endosomes represent an early endocytic intermediate common to a subset of clathrin-derived endocytic vesicles and participate in regulation of trafficking and signaling of growth factor receptors (Zoncu *et al.*, 2009). As a first step to dissecting the BDNF–TrkB endocytic pathway controlling ERK signaling kinetics, we tested whether pTrk enters the endocytic trafficking pathway via APPL1 endosomes in hippocampal neurons after BDNF stimulation. Confocal microscopy revealed a high degree of colocalization between them upon BDNF addition (Figure 5A), indicating that activated TrkB associates with APPL1 endosomes. A high degree of colocalization between pERK1/2 and APPL1 on vesicular structures was also detected upon BDNF treatment (Figure 5A).

To further confirm the endocytic trafficking of BDNF–TrkB via APPL1 endosomes, we performed immunogold labeling on mouse hippocampal sections with antibodies to pTrk and APPL1 (Figure 5, B–D′). It is intriguing that 98 ± 0.9% of pTrk-immunolabeled structures were colabeled with antibodies to APPL1; conversely, 50 ± 3.8% of APPL1-positive structures were also positive for pTrk (Figure 5E). These results suggest that the vast majority of pTrk signaling vesicles traffic through APPL1 endosomes, whereas APPL1 endosomes also serve as endocytic intermediate for other types of cargoes.

Binding of BDNF induces transphosphorylation of the Tyr-515 site on TrkB, which provides a docking site for the signaling adaptor Shc to further activate ERK1/2 and Akt (Atwal *et al.*, 2000; Liu and Meakin, 2002). To test whether APPL1 interacts with activated TrkB on endocytic vesicles, we performed a coIP assay with HEK293 cells expressing FLAG-tagged TrkB and enhanced GFP (EGFP)–APPL1. It was intriguing that whereas a Y515A point mutant that mimics the nonphosphorylatable version of TrkB at the Y515 site (Segal *et al.*, 1996; Atwal *et al.*, 2000; He *et al.*, 2002; Liu and Meakin, 2002) bound less APPL1 than the wild-type protein, binding between APPL1 and the Y515D mutant that mimics phosphorylated TrkB was greatly increased (Figure 5F), suggesting that phosphorylation of TrkB at the Tyr-515 site enhances its interaction with APPL1 on the vesicular surface. Taken together, these data indicate that APPL1-positive endosomes are involved in endocytic trafficking and signaling of activated TrkB.

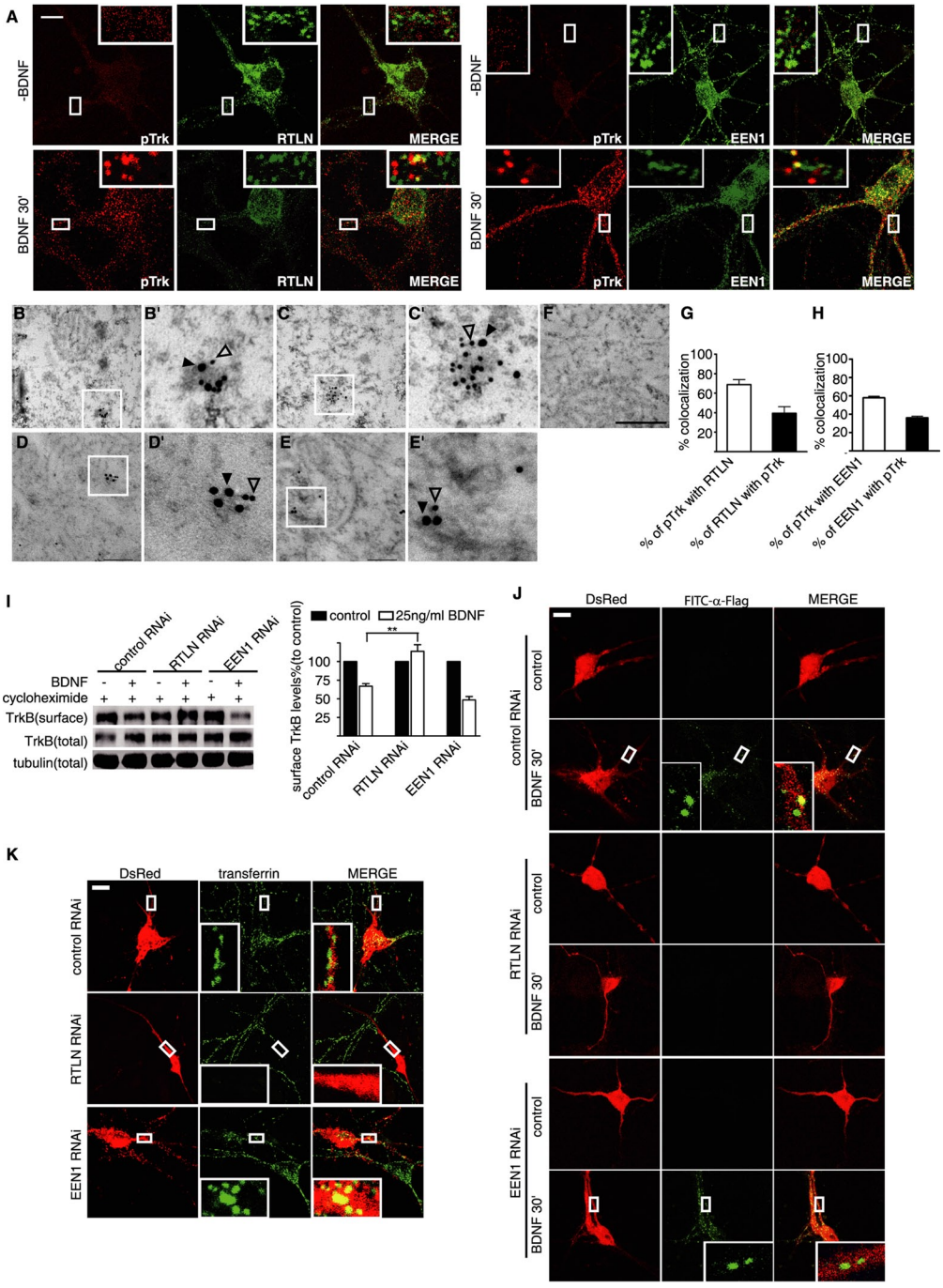

FIGURE 4: Retrolinkin is required for BDNF-triggered TrkB internalization. (A) DIV10 hippocampal neurons were starved for 2 h and incubated with 25 ng/ml BDNF for 30 min, fixed, and immunostained with antibodies to pTrk and retrolinkin or endophilin A1. Scale bar, 10 μm. (B, C) Representative examples of double immunogold labeling of adult mouse hippocampus with antibodies to pTrk (18 nm) and retrolinkin (12 nm). (B′, C′) Higher magnification of boxed areas in B and C, respectively. (D, E) Representative examples of double immunoEM labeling of pTrk (18 nm) and endophilin A1 (12 nm). (D′, E′) Higher magnification of boxed areas in D and E, respectively. (F) Negative control with secondary antibodies only. Scale bar, 350 nm in B–F, 100 nm in B′–E′. (G) Quantification of the colocalization between pTrk and retrolinkin in immunoEM. Data represent means ± SEM (n = 3). (H) Quantification of the colocalization between pTrk and endophilin A1 in immunoEM. Data represent means ± SEM (n = 3). (I) Cortical neurons infected with *Lentivirus* expressing shRNA were treated with BDNF (25 ng/ml) for 30 min. TrkB internalization was then measured by cleavable surface biotinylation. Surface TrkB was detected by Western blotting with anti-panTrk. Total TrkB and tubulin were detected by Western blotting of whole-cell lysates. The quantified immunoblot bands are shown (right). Values were normalized to the respective TrkB levels of control (**$p < 0.01$, $n = 3$). (J) Hippocampal neurons transfected with FLAG-TrkB and shRNA expression constructs were treated with BDNF (25 ng/ml) for 30 min. Internalized TrkB was labeled with FITC–α-FLAG and analyzed by confocal microscopy. (K) Hippocampal neurons transfected with shRNA constructs for 3–4 d were starved for 2 h, followed by incubation with 10 μg/ml Alexa Fluor 488–conjugated transferrin for 1 h. Neurons were fixed and analyzed by confocal microscopy. EEN1, endophilin A1; RTLN, retrolinkin.

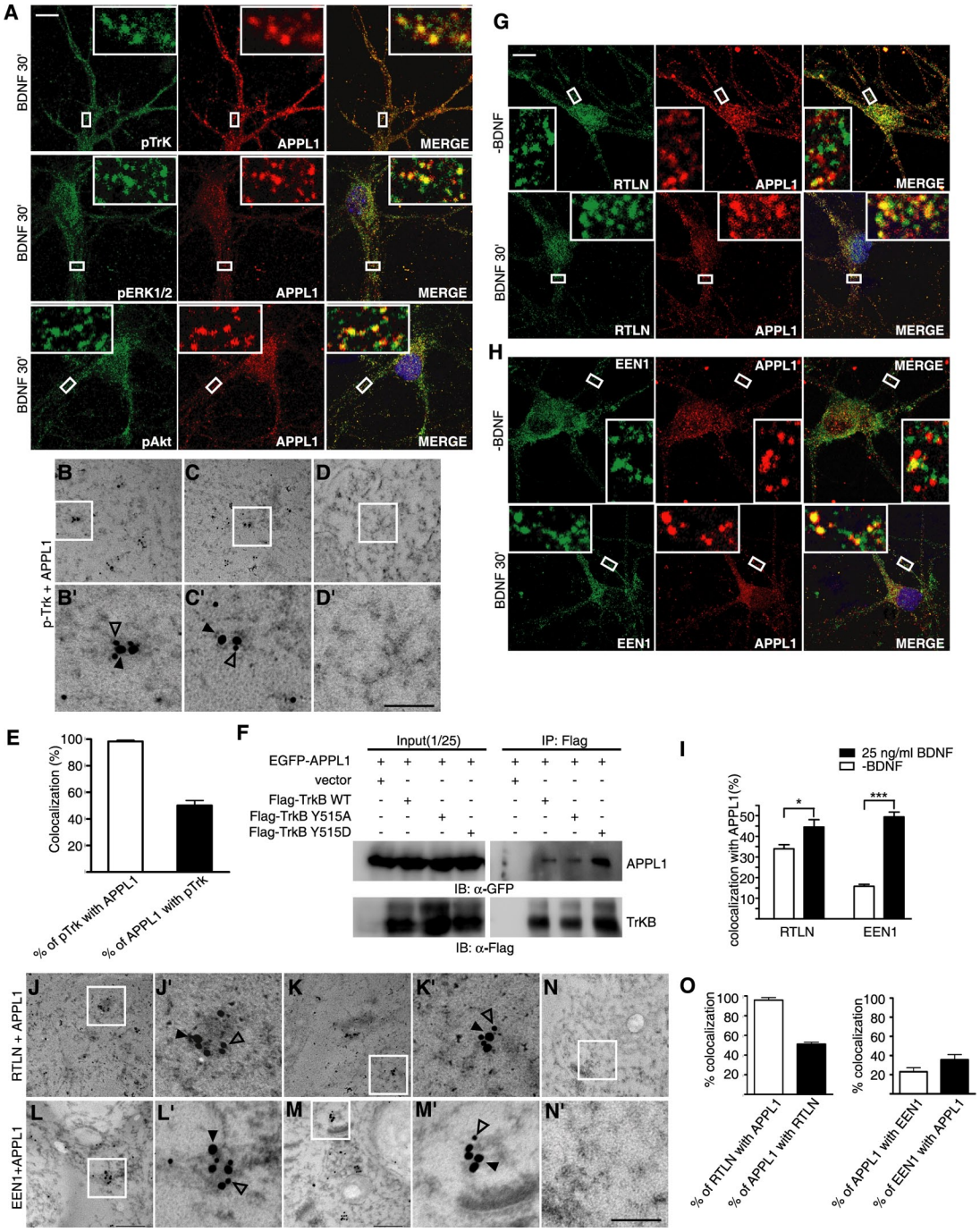

FIGURE 5: Activated TrkB traffic through APPL1 endosomes. (A) Localization of pTrk, pERK1/2, and pAkt to APPL1-positive endosomes. DIV10 hippocampal neurons were starved for 2 h, stimulated with BDNF (25 ng/ml) for 30 min, and double stained with different antibodies. Scale bar, 10 μm. (B, C) Representative examples of double immunogold labeling of adult mouse hippocampus with antibodies to pTrk (18 nm) and APPL1 (12 nm). (D) Negative control with secondary antibodies only. (B′–D′) Higher magnification of boxed areas in B–D, respectively. Scale bar, 350 nm in B–D, 100 nm in B′–D′. (E) Quantification of the colocalization of pTrk with APPL1 in immunoEM. Data represent means ± SEM (n = 3–5). (F) CoIP of lysates of HEK293 cells overexpressing FLAG-tagged TrkB and EGFP-APPL1 with immobilized FLAG antibody. Immunoblot was probed with antibodies to FLAG and GFP. (G, H) The colocalization of retrolinkin or endophilin A1 with APPL1 was increased upon BDNF treatment. DIV10 hippocampal neurons were starved for 2 h, stimulated with BDNF (25 ng/ml) for 30 min, and double stained with antibodies to APPL1 and retrolinkin or endophilin A1. Scale bar, 10 μm. (I) Quantification of the colocalization between APPL1 and retrolinkin or endophilin A1. Data represent means ± SEM (n = 12–20) (*$p < 0.05$; ***$p < 0.001$). (J, K) Representative examples of double immunogold labeling of adult mouse hippocampus with antibodies to retrolinkin (18 nm) and APPL1 (12 nm). (L, M) Representative examples of double immunogold labeling with antibodies to endophilin A1 (12 nm) and APPL1 (18 nm). (N) Negative control with secondary antibodies only. (J′–N′) Higher magnification of boxed area in J–N, respectively. Scale bar, 350 nm in J–N, 100 nm in J′–N′. (O) Quantification of the colocalization of retrolinkin or endophilin A1 with APPL1 in immunoEM. Data represent means ± SEM (n = 3–5). EEN1, endophilin A1; RTLN, retrolinkin.

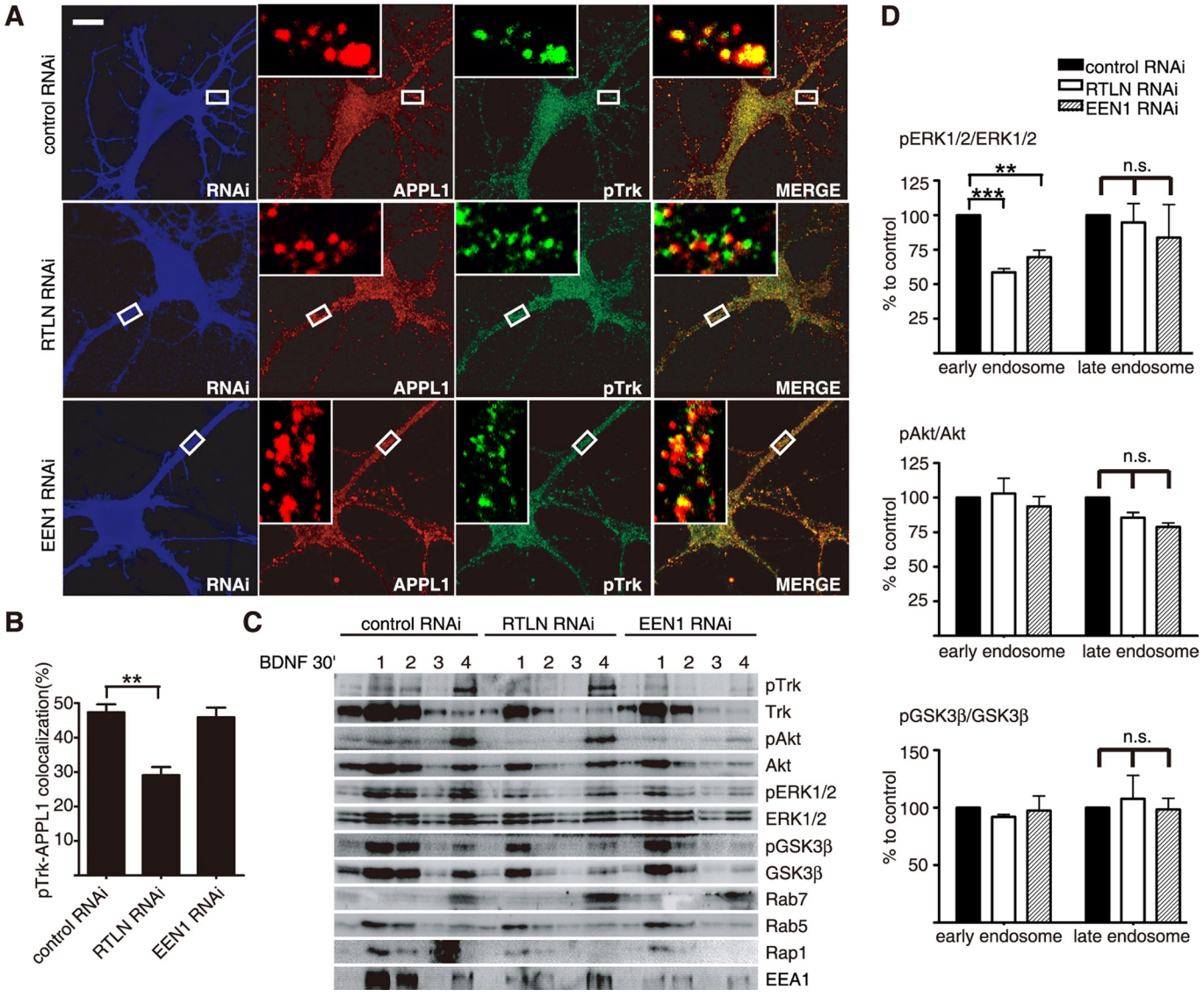

FIGURE 6: Retrolinkin and endophilin A1 are required for BDNF-induced acute ERK activation from early endosomes. (A) Hippocampal neurons transfected with shRNA constructs were treated with BDNF (25 ng/ml) for 30 min, fixed, and immunostained with antibodies to pTrk, APPL1, and RFP. (B) Quantification of the colocalization between pTrk and APPL1 in A. Data represent means ± SEM (**$p < 0.005$, $n = 30–35$). (C) Cortical neurons infected with *Lentivirus* expressing shRNA were stimulated with BDNF (25 ng/ml) and subjected to subcellular fractionation. The early (fractions 1 and 2) and late (fractions 3 and 4) endosomal fractions were extracted after centrifugation with an Opti-Prep discontinuous gradient and analyzed by immunoblotting. Rab5 and EEA1 served as markers for early endosomes, and Rab7 served as a marker for late endosomes. (D) Quantitative analysis of the immunoblot bands in C. Data represent means ± SEM (**$p < 0.01$; ***$p < 0.001$, $n = 3$). EEN1, endophilin A1; n.s., not significant; RTLN, retrolinkin.

To test whether retrolinkin and/or endophilin A1 are involved in pTrk endocytic vesicle trafficking through APPL1 endosomes, first we performed immunofluorescence staining analyses and found that colocalization of both retrolinkin and endophilin A1 with APPL1 in hippocampal neurons increased upon BDNF stimulation (Figure 5, G–I). Double immunogold labeling also revealed that both proteins colocalized with APPL1 on vesicular structures, with 96 ± 2.6% of retrolinkin-positive structures also positive for APPL1, and 36 ± 5.5% of endophilin A1-immunolabeled structures colabeled with antibodies to APPL1 (Figure 5, J–M′ and O), suggesting that a large fraction of retrolinkin-associated vesicular cargoes traffics through APPL1 endosomes, whereas only a subset of endophilin A1–associated vesicles traffics through APPL1.

Suppression of retrolinkin or endophilin A1 expression inhibits BDNF-induced ERK activation from early endosomes

To further investigate the role(s) of retrolinkin and endophilin A1 in pTrk endocytic trafficking through APPL1 endosomes, we suppressed their expression in cultured hippocampal neurons. Consistent with our findings that retrolinkin depletion blocks BDNF-induced TrkB endocytosis (Figure 4, I and J), knockdown of retrolinkin caused a decrease in colocalization of pTrk with APPL1 (Figure 6, A and B). In contrast, endophilin A1 knockdown did not inhibit localization of pTrk to APPL1 vesicles (Figure 6, A and B), indicating that retrolinkin, not endophilin A1, is required for entry of pTrk into APPL1 endosomes.

To verify that ERK activation relies on pTrk early endocytic trafficking, we analyzed endosomal membrane fractions prepared from

BDNF-stimulated cortical neurons and found that most pERK1/2 signals were detected in the early endosomal fractions 30 min after BDNF addition and that knockdown of retrolinkin or endophilin A1 caused a decrease in pERK1/2 levels in the early but not late endosomal fractions (Figure 6, C and D), indicating that both retrolinkin and endophilin A1 are required for BDNF-induced ERK activation on early endosomes. Taken together, these results indicate that retrolinkin and endophilin A1 mediate BDNF–TrkB trafficking and signaling from early endosomes via APPL1 transport vesicles.

Retrolinkin is required for recruitment of endophilin A1 to pTrk-, APPL1-positive endosomes

Because both retrolinkin and endophilin A1 are required for dendrite development as well as ERK signaling, and retrolinkin but not endophilin A1 is required for BDNF-induced TrkB endocytosis, we reasoned that endophilin A1 functions downstream of retrolinkin in BDNF–TrkB endocytic trafficking. Confocal analysis revealed that retrolinkin knockdown greatly reduced the colocalization between endophilin A1 and pTrk puncta (Figure 7, A and C), whereas endophilin A1 knockdown did not have an obvious effect on the colocalization between retrolinkin and pTrk (Figure 7, B and C), indicating that recruitment of endophilin A1 to pTrk-positive vesicles requires retrolinkin activity. Moreover, quantification of double immunofluorescence staining analysis with antibodies to pERK1/2 and retrolinkin showed less colocalization between pERK1/2 and retrolinkin than that between pERK1/2 and endophilin A1 (Figure 3, F–H). These results strongly suggest that endophilin A1 acts downstream of retrolinkin to mediate the maturation of pTrk early endocytic vesicles to endosomes that serve as activation sites for ERK1/2.

The coIP assay did not detect an interaction between endophilin A1 and APPL1 (Figure 7D), indicating that its recruitment to APPL1 endosomes does not require direct binding to APPL1. Knockdown of retrolinkin expression reduced the colocalization of endophilin A1 with APPL1 endosomes (Figure 7, E and F), whereas endophilin A1 knockdown did not affect the distribution of retrolinkin to APPL1 vesicles (Figure 7, G and H). Thus retrolinkin is required for BDNF-induced recruitment of endophilin A1 to APPL1 endosomes.

DISCUSSION

In this study, we presented evidence that retrolinkin, previously found to play a role in retrograde axonal transport in sensory neurons, also functions in BDNF–TrkB trafficking and signaling in CNS neurons. Retrolinkin directly interacts with endophilin A1, and both proteins are required for BDNF–TrkB early endocytic trafficking and spatiotemporal regulation of BDNF-induced ERK activation. Retrolinkin not only functions in endocytosis of BDNF–TrkB, but it also recruits endophilin A1 to pTrk-, APPL1-positive endosomes to regulate acute activation of ERK on early endosomes.

On the basis of our findings, we propose that retrolinkin and endophilin A1 are regulators of BDNF–TrkB endocytic trafficking and that they control dendrite outgrowth by selectively controlling ERK signaling kinetics (Figure 8). In this model, upon cell surface entry of BDNF–TrkB through retrolinkin-dependent, receptor-mediated endocytosis, the internalized cargo carrying activated TrkB enters the endocytic pathway and forms APPL1-positive vesicles. Further conversion of pTrk-, APPL1-positive vesicles to signaling endosomes requires endophilin A1, which is recruited by retrolinkin. The activated TrkB receptor thus traffics through APPL1 endosomes to trigger acute activation of ERK1/2 through unknown mechanisms. Several lines of evidence support this model. First, BDNF-triggered TrkB endocytosis requires retrolinkin activity, and there is a high degree of colocalization between retrolinkin and pTrk/APPL1 on vesicular structures upon BDNF stimulation. Second, localization of pTrk to APPL1 vesicles, as well as localization of endophilin A1 to pTrk-, APPL1-positive vesicles, requires retrolinkin activity, indicating that these two proteins act sequentially along the pTrk endocytic trafficking pathway. Third, depletion of retrolinkin or endophilin A1 not only inhibits transient increase in pERK1/2 levels after BDNF stimulation, but it also results in a decrease in pERK1/2 levels on early endosomes, indicating that acute ERK signaling from early endosomes is regulated by these two proteins.

Previous studies established that ERK signaling is required for neurotrophin-induced neurite outgrowth. ERK activates phospholipase D2 to produce the pleiotropic signaling lipid messenger phosphatidic acid and regulates actin-based membrane dynamics (Watanabe *et al.*, 2004). ERK also regulates GSK-3–mediated phosphorylation of paxillin to modulate cytoskeleton rearrangement in neurite extension (Cai *et al.*, 2006). The present report is the first to demonstrate that activated TrkB entering a specific endocytic trafficking pathway can induce acute ERK activation in CNS neurons, and blockade of this pathway also blocks BDNF-induced dendrite outgrowth. Our results are consistent with a study showing that internalization of activated Trk regulates the strength and duration of NGF-induced ERK signaling in PC12 cells (Zhang *et al.*, 2000). Because dendrite outgrowth requires membrane supply and active cytoskeleton reorganization, an acute local activation of ERK may provide signaling cues for the cell to respond quickly to extrinsic signals such as neurotrophins for dendritogenesis.

In addition, our study is the first to demonstrate that endophilin A1, previously known to play a role in synaptic vesicle recycling and synaptic transmission at the presynaptic site (Ringstad *et al.*, 1999; Gad *et al.*, 2000; Guichet *et al.*, 2002; Verstreken *et al.*, 2002, 2003; Schuske *et al.*, 2003; Chowdhury *et al.*, 2006), also functions in the postendocytic trafficking and signaling of BDNF and regulates dendritic morphogenesis. Of interest, a recent study reported that endophilin B1, another member of the endophilin family, interacts with TrkA and regulates the postendocytic trafficking and signaling of NGF–TrkA in PC12 cells and SCG neurons (Wan *et al.*, 2008). Suppression of endophilin B1 expression leads to precocious targeting of NGF to late endosomes and lysosomes, accelerating NGF degradation and reducing TrkA signaling on endosomes (Wan *et al.*, 2008). Taken together, the endophilins might coordinate with each other to mediate trafficking of neurotrophin–Trk complexes at different stages. Alternatively, they might serve distinct functions in the endocytic pathways of neurotrophins in different neuronal cell types.

In summary, our observation that retrolinkin- and endophilin A1–mediated endocytic trafficking of activated TrkB selectively regulates signaling kinetics of ERK corroborates the regulatory role of receptor location in the temporal patterns of signaling cascades. That suppression of their activities causes no change in sustained ERK activation suggests that alternative endocytic pathway(s) are involved in addition to TrkB endosomal entry via APPL1 endocytic intermediates. It remains to be determined how retrolinkin mediates TrkB endocytosis since there is no evidence for direct physical interaction between these two proteins. Moreover, mechanisms for conversion of pTrk-, APPL1-positive endocytic vesicles to signaling endosomes are unclear. Given that both endophilin A1 and APPL1 are BAR-domain proteins, they might play a role in mediating conversion of vesicles through 1) membrane deformation via their membrane curvature–modulating BAR domains (Doherty and McMahon, 2009) and/or 2) by recruiting more regulatory factors via their protein–protein interacting SH3 and PH domains, respectively. Further work will be needed to

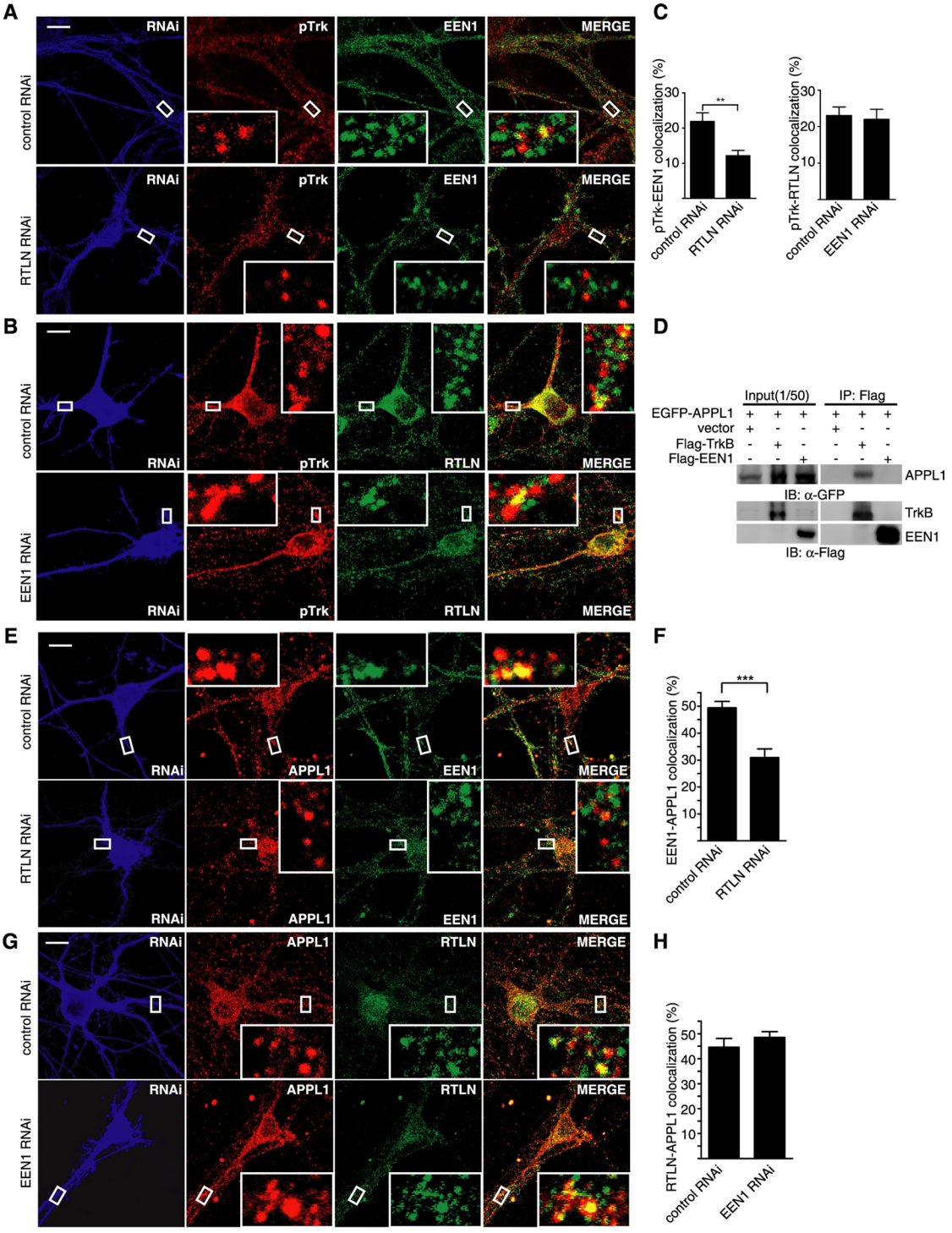

FIGURE 7: Recruitment of endophilin A1 to APPL1 endosomes requires retrolinkin activity. (A) Hippocampal neurons transfected with the retrolinkin shRNA construct were starved for 2 h, treated with BDNF (25 ng/ml), fixed, and immunostained with antibodies to pTrk, endophilin A1, and RFP. Quantification of colocalization is shown (right). Data represent means ± SEM (n = 15) (**p < 0.01). (B) Hippocampal neurons transfected with the endophilin A1 shRNA construct were stimulated with BDNF and immunostained with antibodies to pTrk, retrolinkin, and RFP. (C) Quantification of colocalization between pTrk and endophilin A1 or retrolinkin, respectively. Data represent means ± SEM (n = 15). Scale bar, 10 μm. (D) CoIP of HEK293 cells overexpressing EGFP-APPL1 and FLAG-TrkB or FLAG-endophilin A1. Cell lysates were incubated with immobilized FLAG antibody. Immunoblot was probed with antibodies to FLAG and GFP. (E) Hippocampal neurons transfected with control or retrolinkin shRNA construct were immunostained with antibodies to endophilin A1, APPL1, and RFP after BDNF treatment. (F) Quantification of the colocalization between endophilin A1 and APPL1. Data represent means ± SEM (***p < 0.001; n = 15). (G) Hippocampal neurons transfected with the control or endophilin A1 shRNA construct were immunostained with antibodies to retrolinkin, APPL1, and RFP after BDNF treatment. Scale bar, 10 μm. (H) Quantification of the colocalization between retrolinkin and APPL1. Data represent means ± SEM (n = 15). EEN1, endophilin A1; RTLN, retrolinkin.

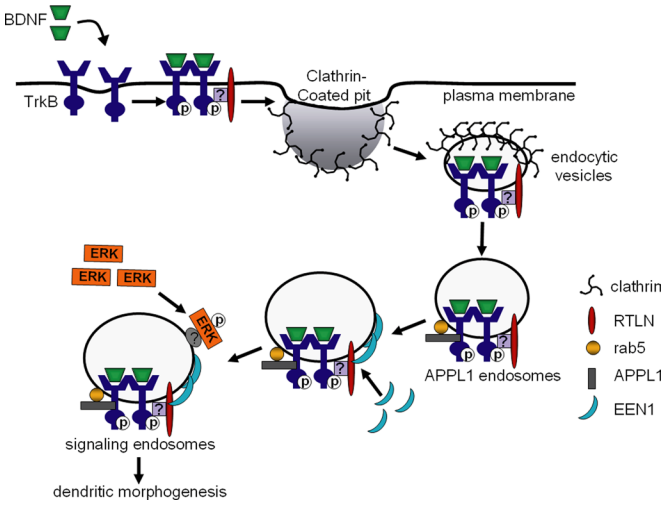

FIGURE 8: Working model for a role of retrolinkin and endophilin A1 in BDNF–TrkB endocytic trafficking and downstream signaling pathways. TrkB receptors are activated upon binding to BDNF, and the internalization of BDNF–TrkB complex into endocytic vesicles is mediated by retrolinkin through unknown mechanisms. After TrkB-positive endocytic vesicles mature into APPL1 endosomes, endophilin A1 is recruited to these endosomes by retrolinkin, and then downstream effectors such as ERK1/2 are recruited to signaling endosomes for acute activation. EEN1, endophilin A1; RTLN, retrolinkin.

delineate the precise sorting/transport pathways mediated by retrolinkin and endophilin A1 and the molecular mechanisms underlying the coordinated actions of the endocytic and sorting machineries in the spatiotemporal regulation of BDNF–TrkB signal transduction. Phenotypic analyses of retrolinkin knockout mice would also enhance our knowledge on its in vivo functions and membrane traffic–regulated signaling cascades under physiological conditions.

MATERIALS AND METHODS

DNA constructs and shRNAs

The FLAG-TrkB expression construct was a generous gift from Zhe-Yu Chen (Shandong University, Jinan, China). FLAG-TrkB Y515A and FLAG-TrkB Y515D were generated by mutating TAC to GCC and TAC to GAT, respectively. The human retrolinkin coding sequence (amino acids [aa] 31–575) was amplified from HeLa cell cDNA and inserted into the yeast expression vector pGBKT7 (Clontech, Mountain View, CA). Mouse endophilin A1 cDNA was amplified from a mouse brain cDNA library and inserted into pGBKT7. The pGADT7-RTLN (aa 31–460), pGEX4T-1-RTLN (aa 31–460), pGEX4T-1-RTLN (aa 489–574), pGEX4T-1-RTLN (aa 31–169), pGEX4T-1-RTLN (aa 173–373), pGEX4T-1-RTLN (aa 271–373), and pET28a-RTLN (aa 31–460) were constructed with mouse retrolinkin cDNA, and pET28a-EEN1, pGEX4T-1-EEN1, pGEX4T-1-EEN1ΔBAR (Δaa 6–242), pGEX4T-1-EEN1ΔSH3 (Δaa 295–346), and pGEX4T-1-EEN1 SH3 (aa 295–346) were constructed with mouse endophilin A1 (EEN1) cDNA using standard molecular biology methods. The FLAG-tagged retrolinkin and endophilin A1 were inserted into lentiviral vector (a gift from Tieshan Tang, Institute of Zoology, Chinese Academy of Sciences, Beijing, China) between *Eco*RI and *Bam*HI, respectively. To construct shRNAs, the sense and antisense primers (as follows) were annealed, and then the annealing oligos were inserted into pLL3.7.4 between *Xho*I and *Hpa*I sites.

Mouse retrolinkin shRNA #1 (nucleotides [nt] 283–301):

TGACACCACGTCTACAGTGATTCAAGAGATCACTGTAGACGTGGTGTCTTTTTTC and TCGAGAAAAAAGACACCACGTCTACAGTGATCTCTTGAATCACTGTAGACGTGGTGTCA

Mouse retrolinkin shRNA#2 (nt 1505–1523):

TACAACCTGAGCTACTGGAAttcaagagaTTCCAGTAGCTCAGGTTGTTTTTTTC and TCGAGAAAAAAACAACCTGAGCTACTGGAAtctcttgaaTTCCAGTAGCTCAGGTTGTA

Mouse endophilin A1 shRNA (nt 384–402):

TggactcattggacatggaattcaagagaTTCCATGTCCAATGAGTCCTTTTTTC and TCGAGAAAAAAGGACTcattggacatggaatctcttgaaTTCCATGTCCAATGAGTCCA

Control shRNA (Mouse retrolinkin scrambled shRNA):

TGACAtCACGgCTAtAGcGATTCAAGAGATCGCTATAGCCGTGATGTCTTTTTTC and TCGAGAAAAAAGACATCACGGCTATAGCGATCTCTTGAATCGCTATAGCCGTGATGTCA

The FLAG-tagged, shRNA-resistant retrolinkin expression construct was generated by mutating ACAACCTGAGCTACTGGAA (nt 1505–1523 of retrolinkin coding region) to ACAACCTGTCCTACTGGAA without changing amino acid sequence. The FLAG-tagged, shRNA-resistant endophilin A1 expression construct was generated by mutating GGACTCATTGGACATGGAA (nt 384–402 of endophilin A1 coding region) to GGACTCTCTGGACATGGAA. Mutated retrolinkin or endophilin A1 cDNA was inserted into a lentiviral expression vector between *Eco*RI and *Bam*HI sites. Full-length mouse APPL1 cDNA was amplified from a mouse brain cDNA and inserted into pEGFP-C3 (Clontech). All constructs were verified by sequencing.

Antibodies

Rabbit and guinea pig polyclonal antibodies against mouse retrolinkin were raised as described previously (Liu *et al.*, 2007). Anti–endophilin A1 antisera were obtained by immunization of guinea pigs with histidine (His)-tagged endophilin A1 full-length protein expressed and purified from *Escherichia coli*. Antibodies were affinity purified with the antigen immobilized on AminoLink agarose gel beads (Affi-Gel; Bio-Rad Laboratories, Hercules, CA). Antibodies used in the present study include antibodies against phospho-Trk (Tyr-490), ERK1/2, phospho-ERK1/2 (Thr-202/Tyr-204), GSK3β, phospho-GSK3β (Ser-9), Akt, phospho-Akt (Ser-473), PLCγ, phospho-PLCγ (Cell Signaling Technology, Beverly, MA), βIII-tubulin, MAP2 (Chemicon, Temecula, CA), TAU1 (Millipore, Billerica, CA), Rab5b, Rab7, APPL1, pan-Trk, TrkB (Santa Cruz Biotechnology, Santa Cruz, CA), α-tubulin, β-actin, monoclonal anti-FLAG M2-FITC (Sigma-Aldrich, St. Louis, MO), Rap1, and EEA1 (BD Biosciences, San Diego, CA). Secondary antibodies for immunofluorescence staining were from Molecular Probes (Invitrogen, Carlsbad, CA). Colloidal gold secondary antibodies for immunoEM were from Jackson ImmunoResearch Laboratories (West Grove, PA).

Yeast two-hybrid screen and assays

Yeast two-hybrid screen and assays using the Matchmaker Gal4 system (Clontech) were performed following the manufacturer's protocols and as described (Hong *et al.*, 2009). Retrolinkin has two transmembrane (TM) domains, with aa 12–29 as TM1 and aa 468–488 as TM2 (Figure 2A). We used a truncated form of human retrolinkin (aa 31–574) with the removal of the first 30 amino acids as bait to minimize the possibility of retrolinkin targeting to membrane instead of the nucleus. Protein–protein interaction was examined by growth test of yeast transformants on SD medium lacking leucine, tryptophan, adenine, and histidine (SD-Leu-Trp-Ade-His) and containing 2 mg/ml X-α-Gal. The AH109 strain cotransformed with control vectors pGBKT7-53 and pTD1-1 served as positive control.

GST pull-down assays

An amount of 5 μg of GST-tagged retrolinkin conjugated with glutathione–Sepharose beads was incubated with 1 μg of His-tagged endophilin A1 in binding buffer (20 mM Tris-HCl [pH 7.5], 150 mM NaCl, 5 mM EDTA, 1% NP-40, and bovine serum albumin [BSA; 25 mg/ml]) for 1 h at 4°C. Beads were washed five times with Tris-buffered saline (TBS) and boiled in SDS sample buffer.

Immunoprecipitation

Adult mouse brain or primary cortical neurons were homogenized in 1 ml of cold homogenization buffer (50 mM Tris-Cl, pH 7.4, 20 mM 4-(2-hydroxyethyl)-1-piperazineethanesulfonic acid, pH 7.4, 150 mM NaCl, 1% NP-40, 1 mM phenylmethylsulfonyl fluoride [PMSF], and 1× protease inhibitors). Lysates were centrifuged at 12,000 × *g* for 15 min, and the supernatant was incubated with antibodies (5 μg) at 4°C, followed by incubation with Protein A/G Sepharose (Santa Cruz Biotechnology) preequilibrated in lysis buffer overnight at 4°C. Precipitates were washed five times with ice-cold TBS (50 mM Tris-Cl, pH 7.4, 150 mM NaCl, 0.1% Triton X-100). Complexes were eluted from the Protein A/G Sepharose in 2× SDS sample buffer (100 mM Tris-Cl, pH 6.8, 4% SDS, 0.2% bromophenol blue, 20% [vol/vol] glycerol, 10% [vol/vol] 2-mercaptoethanol) and subjected to SDS–PAGE and immunoblotting. Membrane IP was performed with the membrane fractions (P100) of brain lysates after ultracentrifugation at 100,000 × *g* for 1 h.

Western blotting of BDNF-induced activation of downstream effectors

DIV10 cortical neurons were starved in MEM for 2 h, incubated with BDNF (25 ng/ml) for various time points. Cells were harvested and lysed in lysis buffer (50 mM Tris-Cl, pH 7.4, 150 mM NaCl, 1% Triton X-100, 1 mM Na_3NO_4, 1 mM PMSF). Proteins separated by SDS–PAGE were then transferred onto polyvinylidene fluoride membrane (Millipore) and probed with various antibodies. Immunoblots were imaged with an Epichemi3 Darkroom system (UVP BioImaging Systems, Upland, CA). For densitometric analysis, immunoreactive bands were quantified using ImageJ (National Institutes of Health, Bethesda, MD). All experiments were carried out at least in triplicate.

Neuronal culture, transfection, and viral infection

Hippocampi and cortex were dissected from embryonic day 15.5 BALB/c mice, dissociated with 0.25% trypsin in Hank's balanced salt solution without Ca^{2+} and Mg^{2+} at 37°C for 15 min, triturated in DMEM, 10% F12, and 10% fetal bovine serum. Hippocampal neurons were plated on coverslips coated with 0.1 mg/ml poly-D-lysine in 24-well plates at a cell density of 5×10^5 cells/ml. Cortical neurons were plated in six-well, 12-well, or 10-cm plates coated with 0.1 mg/ml poly-D-lysine at a cell density of 2×10^6 cells/ml. The medium was changed to the serum-free medium (Neurobasal media supplemented with 2% B27 supplement, GlutaMAX, Fungizone [Gibco, Invitrogen], and gentamicin [Amresco, Solon, OH]) 4 h after plating. For neuronal morphology and immunofluorescence staining, neurons were transfected with Lipofectamine 2000 (Invitrogen) following the manufacturer's instructions. For Western blotting, neurons were infected with *Lentivirus* prepared from HEK293T cells.

Immunofluorescence microscopy and image analyses

Primary hippocampal neurons were rinsed with phosphate-buffered saline (PBS) and fixed with 4% paraformaldehyde (PFA) for 15 min at room temperature. Cells were blocked with PBS containing 1% BSA and 0.4% Triton X-100 for 30 min. Primary antibodies were incubated for 1 h at room temperature or overnight at 4°C, and appropriate secondary antibodies conjugated with Alexa Fluor 488, Alexa Fluor 594, or Alexa Fluor 647 were used for detection. Confocal images were obtained using the Spectral Imaging Confocal Microscope Digital Eclipse C1Si (Nikon, Tokyo, Japan) equipped with 408-nm diode, 457/477/488/514-nm Ar, 543-nm HeNe, and 640-nm lasers. Images were acquired using a 40× S Fluor numerical aperture (NA) 1.30 oil objective or a 100× Plan Apochromat VC NA 1.40 oil objective and analyzed with the NIS-Elements AR software provided by Nikon.

To quantify the colocalization of proteins (taking pTrk and APPL1 as examples) on vesicular structures in dendrites of shRNA-expressing cells, the dsRed image was used to label neurons transfected with control, retrolinkin (RTLN), or EEN1 shRNA construct. A total pTrk-positive-vesicles mask was derived from the fluorescence image (Alexa Fluor 488) by subtracting the background for each cell sample such that a faint punctate spot would be captured in the mask but diffuse background labeling would not. Similarly, an APPL1-positive-vesicles mask was derived from the fluorescence image (Alexa Fluor 647). This APPL1-positive-vesicles mask was then superimposed on the pTrk-positive vesicles mask and a polygonal region of interest (ROI) that completely overlapped with dendrites labeled by DsRed was hand drawn. The colocalization of the APPL1-positive vesicles and pTrk-positive vesicles in this ROI was calculated with Mander`s overlap coefficient. Values for colocalization analysis represent mean value ± SE of the mean (SEM).

Quantification of neurite outgrowth

In the morphological study of hippocampal neurons, length of axon and dendrite and size of soma area were measured with NIS-Elements AR. For each measurement, at least 40 cells were counted from randomly selected fields.

Biotinylation assay of surface TrkB

Biotinylation assay of surface TrkB was performed as described (Wan *et al*., 2008). Primary cortical neurons were infected with *Lentivirus* expressing shRNA and cultured for 7 d. DIV10 neurons were starved for 2 h with MEM supplemented with 20 μg/ml cycloheximide, followed by incubation with BDNF (25 ng/ml) in MEM. Cells were then washed three times with ice-cold PBS containing 1 mM $CaCl_2$ and 0.5 mM $MgCl_2$ (PBS-Ca-Mg) and incubated with Sulfo-NHS-LC-biotin (0.25 mg/ml in PBS-Ca-Mg; Pierce, Thermo Fisher Scientific, Rockford, IL) for 1 h at room temperature. The biotinylation reaction was quenched by incubation with PBS-Ca-Mg containing 100 mM glycine for 15 min at 4°C, followed by two washes with PBS-Ca-Mg. Neurons were then lysed in lysis buffer (50 mM Tris-Cl, pH 7.4, 150 mM NaCl, 1% Triton X-100, 1 mM PMSF). After centrifugation at 12,000 × *g* at 4°C for 10 min, the supernatant was incubated with streptavidin beads (Pierce) overnight at 4°C. After extensive washing with TBS (50 mM Tris-Cl, pH 7.4, 150 mM NaCl, 0.1% Triton X-100), bound proteins were eluted in SDS–PAGE sample buffer and subjected to SDS–PAGE and immunoblotting. The immunoblots were also probed with mouse anti–α-tubulin as the loading control.

TrkB internalization assay by fluorescence microscopy

DIV3 hippocampal neurons transfected with the FLAG-TrkB and shRNA construct (FLAG-TrkB:shRNA = 3:1) were grown on glass coverslips. After starvation with MEM for 2 h, DIV7 cells were incubated with 5 μg/ml FITC–anti-FLAG antibody (Sigma-Aldrich) for 30 min at room temperature to selectively label FLAG-tagged TrkB receptors on the plasma membrane. Cells were rinsed with MEM three times

and then incubated with BDNF for 30 min at 37°C. Cells were then quickly washed three times with ice-cold 1× PBS–20 mM EDTA to dissociate fluorescent M1 antibody from residual cell surface receptors. Cells were then fixed with 4% PFA, with the intracellular fluorescence representing the internalized receptors.

Transferrin uptake assay

DIV3 hippocampal neurons were transfected with shRNA construct. After starvation with MEM for 2 h, DIV7 cells were incubated with 10 µg/ml Alexa 488–conjugated transferrin (Invitrogen) for 1 h at 37°C. Cells were then washed once with ice-cold 1× PBS, acid stripped with ice-cold 500 mM NaCl/0.2 N acetic acid in 1× PBS three times, and washed with ice-cold 1× PBS twice before fixation with 4% PFA in 1× PBS.

Subcellular fractionation

Primary cortical neuron fractionation was performed as described by Wu *et al.* (2001). Briefly, BDNF-treated cortical neurons were homogenized in 2 ml of cold homogenization buffer (HB; 250 mM sucrose, 20 mM tricine-NaOH, pH 7.8, 1 mM EDTA, and 2 mM $MgCl_2$). After centrifugation at 800 × g for 10 min, the supernatant was adjusted to 25% OptiPrep with 60% OptiPrep, loaded at the bottom of a centrifuge tube, and overlaid with 2 ml each of 20, 15, 10, and 5% OptiPrep successively in cold HB. After centrifugation at 100,000 × *g* at 4°C for 18 h, membrane fractions were collected from each of four interphases of the gradients.

Immuno–electron microscopy

Tissue preparation and immuno–electron microscopy were conducted as described (Phend *et al.*, 1995). Briefly, adult mouse was anesthetized with 2% pentobarbital sodium and perfusion-fixed with the cold mixture of 0.1% glutaraldehyde (catalog #16220; Electron Microscopy Sciences, Hatfield, PA), 4% PFA (catalog #157-8, Electron Microscopy Sciences), and 0.1% picric acid in phosphate buffer (PB; 0.1 M, pH 7.3). The brain was removed immediately and postfixed in the same fixative for 4 h at 4°C and then stored in 0.1 M PB buffer. Hippocampal tissue blocks were cut with a Vibratome at a thickness of 50 µm and placed in 0.1 M PB buffer. All processing is in glass vials, over ice on a shaker until 100% ethanol . Sections were incubated for 40 min in 1% tannic acid and rinsed twice in maleate buffer (MB), followed by incubation in the dark with 1% uranyl acetate (UAc) in MB for 40 min and rinsed twice in MB. Then sections were incubated for 5 min each in 50 and 70% ethanol and 15 min in freshly prepared 1% *p*-phenylenediamine in 70% ethanol and rinsed twice in 70% ethanol, followed by dehydration for 5 min in 80 and 95% ethanol and twice for 15 min in 100% ethanol, followed by infiltration with 100% LR White for 4 h, changed once and overnight, and then a final change the following morning before embedding. Resin was polymerized at 55°C for 48 h. Ultrasections were collected on 200-mesh nickel grids coated with Formvar membrane. For labeling, grids were blocked for 1 h with Tris-buffered saline containing 50 mM glycine, 1 mg/ml BSA, and 0.1% Triton X-100 (TBS/T), pH 7.6, incubated overnight with primary antibodies (diluted in TBS/T) at 4°C, followed by rinse in 0.1 M PB and transferred to TBS/T, pH 8.2, then incubated overnight with appropriate colloidal gold–conjugated secondary antibodies (Jackson ImmunoResearch Laboratories) diluted with TBS/T, pH 8.2, at 4°C, followed by rinse in 0.1 M PB and incubated in 2% glutaraldehyde for 10 min, then rinsed in doubly distilled H_2O (ddH_2O) and incubated with 2% UAc (diluted with ddH_2O) for 15 min and lead for 2 min, followed by rinse in ddH_2O and dried. Sections were examined with a JEM-1400 transmission electron microscope (JEOL, Tokyo, Japan). For double labeling, quantification was performed using randomly photographed hippocampus areas at a magnification of 30,000 of the various double-labeled preparations; the number of ultrastructures with one size of gold label and with both sizes of gold label was counted. A minimum of 10 pictures per labeling was obtained for analysis. An ultrastructure was considered as positive for the protein studied when a minimum of two gold particles (one size or both sizes) was found. Each quantification included a minimum of 80 labeled structures. The results are presented as the mean ± SEM of at least three independent labeling experiments.

Statistical analysis

Confocal images were analyzed using the NIS-Elements AR 3.1 software provided by Nikon. GraphPad Prism 4 (GraphPad Software, La Jolla, CA) was used for statistical analysis, and Student's *t* test was used to evaluate statistical significance.

ACKNOWLEDGMENTS

We thank Zhe-Yu Chen (Shandong University) and Tieshan Tang (Institute of Zoology, Chinese Academy of Sciences) for generously providing us with reagents. We also thank Li Yu (Tsinghua University, Beijing, China), Dahua Chen (Institute of Zoology, Chinese Academy of Sciences), and Zhe-Yu Chen for critical reading of the manuscript. This work was supported by grants from the National Natural Science Foundation of China (30770675), the Ministry of Science and Technology (2011CB965002), and the Chinese Academy of Sciences Key Project (KSCX2-EW-R-05). J.J.L. is supported by the Chinese Academy of Sciences 100-Talents Program.

REFERENCES

Atwal JK, Massie B, Miller FD, Kaplan DR (2000). The TrkB-Shc site signals neuronal survival and local axon growth via MEK and P13-kinase. Neuron 27, 265–277.

Cai X, Li M, Vrana J, Schaller MD (2006). Glycogen synthase kinase 3- and extracellular signal-regulated kinase-dependent phosphorylation of paxillin regulates cytoskeletal rearrangement. Mol Cell Biol 26, 2857–2868.

Chen ZY, Ieraci A, Tanowitz M, Lee FS (2005). A novel endocytic recycling signal distinguishes biological responses of Trk neurotrophin receptors. Mol Biol Cell 16, 5761–5772.

Chowdhury S, Shepherd JD, Okuno H, Lyford G, Petralia RS, Plath N, Kuhl D, Huganir RL, Worley PF (2006). Arc/Arg3.1 interacts with the endocytic machinery to regulate AMPA receptor trafficking. Neuron 52, 445–459.

Delcroix JD, Valletta JS, Wu C, Hunt SJ, Kowal AS, Mobley WC (2003). NGF signaling in sensory neurons: evidence that early endosomes carry NGF retrograde signals. Neuron 39, 69–84.

Dijkhuizen PA, Ghosh A (2005). BDNF regulates primary dendrite formation in cortical neurons via the PI3-kinase and MAP kinase signaling pathways. J Neurobiol 62, 278–288.

Doherty GJ, McMahon HT (2009). Mechanisms of endocytosis. Annu Rev Biochem 78, 857–902.

Ehlers MD, Kaplan DR, Price DL, Koliatsos VE (1995). NGF-stimulated retrograde transport of trkA in the mammalian nervous system. J Cell Biol 130, 149–156.

Gad H *et al.* (2000). Fission and uncoating of synaptic clathrin-coated vesicles are perturbed by disruption of interactions with the SH3 domain of endophilin. Neuron 27, 301–312.

Grimes ML, Zhou J, Beattie EC, Yuen EC, Hall DE, Valletta JS, Topp KS, LaVail JH, Bunnett NW, Mobley WC (1996). Endocytosis of activated TrkA: evidence that nerve growth factor induces formation of signaling endosomes. J Neurosci 16, 7950–7964.

Guichet A, Wucherpfennig T, Dudu V, Etter S, Wilsch-Brauniger M, Hellwig A, Gonzalez-Gaitan M, Huttner WB, Schmidt AA (2002). Essential role of endophilin A in synaptic vesicle budding at the *Drosophila* neuromuscular junction. EMBO J 21, 1661–1672.

He XP, Minichiello L, Klein R, McNamara JO (2002). Immunohistochemical evidence of seizure-induced activation of trkB receptors in the mossy fiber pathway of adult mouse hippocampus. J Neurosci 22, 7502–7508.

Heerssen HM, Segal RA (2002). Location, location, location: a spatial view of neurotrophin signal transduction. Trends Neurosci 25, 160–165.
Hisata S, Sakisaka T, Baba T, Yamada T, Aoki K, Matsuda M, Takai Y (2007). Rap1-PDZ-GEF1 interacts with a neurotrophin receptor at late endosomes, leading to sustained activation of Rap1 and ERK and neurite outgrowth. J Cell Biol 178, 843–860.
Hong Z, Yang Y, Zhang C, Niu Y, Li K, Zhao X, Liu JJ (2009). The retromer component SNX6 interacts with dynactin p150(Glued) and mediates endosome-to-TGN transport. Cell Res 19, 1334–1349.
Huang EJ, Reichardt LF (2001). Neurotrophins: roles in neuronal development and function. Annu Rev Neurosci 24, 677–736.
Huang EJ, Reichardt LF (2003). Trk receptors: roles in neuronal signal transduction. Annu Rev Biochem 72, 609–642.
Huang SH, Zhao L, Sun ZP, Li XZ, Geng Z, Zhang KD, Chao MV, Chen ZY (2009). Essential role of Hrs in endocytic recycling of full-length TrkB receptor but not its isoform TrkB.T1. J Biol Chem 284, 15126–15136.
Jan YN, Jan LY (2003). The control of dendrite development. Neuron 40, 229–242.
Kaplan DR, Miller FD (2000). Neurotrophin signal transduction in the nervous system. Curr Opin Neurobiol 10, 381–391.
Lin DC, Quevedo C, Brewer NE, Bell A, Testa JR, Grimes ML, Miller FD, Kaplan DR (2006). APPL1 associates with TrkA and GIPC1 and is required for nerve growth factor-mediated signal transduction. Mol Cell Biol 26, 8928–8941.
Liu HY, Meakin SO (2002). ShcB and ShcC activation by the Trk family of receptor tyrosine kinases. J Biol Chem 277, 26046–26056.
Liu JJ, Ding J, Wu C, Bhagavatula P, Cui B, Chu S, Mobley WC, Yang Y (2007). Retrolinkin, a membrane protein, plays an important role in retrograde axonal transport. Proc Natl Acad Sci USA 104, 2223–2228.
Lu B (2003). BDNF and activity-dependent synaptic modulation. Learn Mem 10, 86–98.
Mao X *et al.* (2006). APPL1 binds to adiponectin receptors and mediates adiponectin signalling and function. Nat Cell Biol 8, 516–523.
Marshall CJ (1995). Specificity of receptor tyrosine kinase signaling: transient versus sustained extracellular signal-regulated kinase activation. Cell 80, 179–185.
McAllister AK, Katz LC, Lo DC (1997). Opposing roles for endogenous BDNF and NT-3 in regulating cortical dendritic growth. Neuron 18, 767–778.
McAllister AK, Lo DC, Katz LC (1995). Neurotrophins regulate dendritic growth in developing visual cortex. Neuron 15, 791–803.
Nguyen TT, Scimeca JC, Filloux C, Peraldi P, Carpentier JL, Van Obberghen E (1993). Co-regulation of the mitogen-activated protein kinase, extracellular signal-regulated kinase 1, and the 90-kDa ribosomal S6 kinase in PC12 cells. Distinct effects of the neurotrophic factor, nerve growth factor, and the mitogenic factor, epidermal growth factor. J Biol Chem 268, 9803–9810.
Niblock MM, Brunso-Bechtold JK, Riddle DR (2000). Insulin-like growth factor I stimulates dendritic growth in primary somatosensory cortex. J Neurosci 20, 4165–4176.
Phend KD, Rustioni A, Weinberg RJ (1995). An osmium-free method of epon embedment that preserves both ultrastructure and antigenicity for post-embedding immunocytochemistry. J Histochem Cytochem 43, 283–292.
Philippidou P, Valdez G, Akmentin W, Bowers WJ, Federoff HJ, Halegoua S (2011). Trk retrograde signaling requires persistent, Pincher-directed endosomes. Proc Natl Acad Sci USA 108, 852–857.
Piontek J, Chen CC, Kempf M, Brandt R (1999). Neurotrophins differentially regulate the survival and morphological complexity of human CNS model neurons. J Neurochem 73, 139–146.
Reutens AT, Begley CG (2002). Endophilin-1: a multifunctional protein. Int J Biochem Cell Biol 34, 1173–1177.
Ringstad N, Gad H, Low P, Di Paolo G, Brodin L, Shupliakov O, De Camilli P (1999). Endophilin/SH3p4 is required for the transition from early to late stages in clathrin-mediated synaptic vesicle endocytosis. Neuron 24, 143–154.
Schenck A, Goto-Silva L, Collinet C, Rhinn M, Giner A, Habermann B, Brand M, Zerial M (2008). The endosomal protein Appl1 mediates Akt substrate specificity and cell survival in vertebrate development. Cell 133, 486–497.
Schuske KR, Richmond JE, Matthies DS, Davis WS, Runz S, Rube DA, van der Bliek AM, Jorgensen EM (2003). Endophilin is required for synaptic vesicle endocytosis by localizing synaptojanin. Neuron 40, 749–762.
Segal RA (2003). Selectivity in neurotrophin signaling: theme and variations. Annu Rev Neurosci 26, 299–330.
Segal RA, Bhattacharyya A, Rua LA, Alberta JA, Stephens RM, Kaplan DR, Stiles CD (1996). Differential utilization of Trk autophosphorylation sites. J Biol Chem 271, 20175–20181.
Traverse S, Gomez N, Paterson H, Marshall C, Cohen P (1992). Sustained activation of the mitogen-activated protein (MAP) kinase cascade may be required for differentiation of PC12 cells. Comparison of the effects of nerve growth factor and epidermal growth factor. Biochem J 288, 351–355.
Varsano T, Dong MQ, Niesman I, Gacula H, Lou X, Ma T, Testa JR, Yates JR 3rd, Farquhar MG (2006). GIPC is recruited by APPL to peripheral TrkA endosomes and regulates TrkA trafficking and signaling. Mol Cell Biol 26, 8942–8952.
Verstreken P, Kjaerulff O, Lloyd TE, Atkinson R, Zhou Y, Meinertzhagen IA, Bellen HJ (2002). Endophilin mutations block clathrin-mediated endocytosis but not neurotransmitter release. Cell 109, 101–112.
Verstreken P, Koh TW, Schulze KL, Zhai RG, Hiesinger PR, Zhou Y, Mehta SQ, Cao Y, Roos J, Bellen HJ (2003). Synaptojanin is recruited by endophilin to promote synaptic vesicle uncoating. Neuron 40, 733–748.
Wan J, Cheung AY, Fu WY, Wu C, Zhang M, Mobley WC, Cheung ZH, Ip NY (2008). Endophilin B1 as a novel regulator of nerve growth factor/ TrkA trafficking and neurite outgrowth. J Neurosci 28, 9002–9012.
Watanabe H, Yokozeki T, Yamazaki M, Miyazaki H, Sasaki T, Maehama T, Itoh K, Frohman MA, Kanaho Y (2004). Essential role for phospholipase D2 activation downstream of ERK MAP kinase in nerve growth factor-stimulated neurite outgrowth from PC12 cells. J Biol Chem 279, 37870–37877.
Wu C, Lai CF, Mobley WC (2001). Nerve growth factor activates persistent Rap1 signaling in endosomes. J Neurosci 21, 5406–5416.
Xu B, Zang K, Ruff NL, Zhang YA, McConnell SK, Stryker MP, Reichardt LF (2000). Cortical degeneration in the absence of neurotrophin signaling: dendritic retraction and neuronal loss after removal of the receptor TrkB. Neuron 26, 233–245.
Yang L, Lin HK, Altuwaijri S, Xie S, Wang L, Chang C (2003). APPL suppresses androgen receptor transactivation via potentiating Akt activity. J Biol Chem 278, 16820–16827.
Zhang Y, Moheban DB, Conway BR, Bhattacharyya A, Segal RA (2000). Cell surface Trk receptors mediate NGF-induced survival while internalized receptors regulate NGF-induced differentiation. J Neurosci 20, 5671–5678.
Zheng J *et al.* (2008). Clathrin-dependent endocytosis is required for TrkB-dependent Akt-mediated neuronal protection and dendritic growth. J Biol Chem 283, 13280–13288.
Zoncu R, Perera RM, Balkin DM, Pirruccello M, Toomre D, De Camilli P (2009). A phosphoinositide switch controls the maturation and signaling properties of APPL endosomes. Cell 136, 1110–1121.